

Article

Unnamed Pt(Cu_{0.67}Sn_{0.33}) from the Bolshoy Khailyk River, Western Sayans, Russia, and a Review of Related Compounds and Solid Solutions

Andrei Y. Barkov ^{1,*}, Luca Bindi ², Erick A. Juárez-Arellano ³, Nobumichi Tamura ⁴, Gennadiy I. Shvedov ⁵, Chi Ma ⁶ and Robert F. Martin ⁷

- ¹ Research Laboratory of Industrial and Ore Mineralogy, Cherepovets State University, Cherepovets 162600, Russia
² Dipartimento di Scienze della Terra, Università degli Studi di Firenze, I-50121 Firenze, Italy; luca.bindi@unifi.it
³ Instituto de Química Aplicada, Universidad del Papaloapan, Circuito Central 200, Parque Industrial, Tuxtpec 68301, Oaxaca, Mexico; eajuarez@unpa.edu.mx
⁴ Advanced Light Source, Lawrence Berkeley National Laboratory, Berkeley, CA 94720-8229, USA; ntamura@lbl.gov
⁵ Institute of Mining, Geology and Geotechnology, Siberian Federal University, Krasnoyarsk 660025, Russia; g.shvedov@mail.ru
⁶ Division of Geological and Planetary Sciences, California Institute of Technology, Pasadena, CA 91125, USA; chima@caltech.edu
⁷ Department of Earth and Planetary Sciences, McGill University, Montreal, QC H3A 0E8, Canada; robert.martin@mcgill.ca
* Correspondence: ore-minerals@mail.ru



Citation: Barkov, A.Y.; Bindi, L.; Juárez-Arellano, E.A.; Tamura, N.; Shvedov, G.I.; Ma, C.; Martin, R.F. Unnamed Pt(Cu_{0.67}Sn_{0.33}) from the Bolshoy Khailyk River, Western Sayans, Russia, and a Review of Related Compounds and Solid Solutions. *Minerals* **2021**, *11*, 1240. <https://doi.org/10.3390/min1111240>

Academic Editors: Mark D. Welch and Sytle M. Antao

Received: 11 October 2021
Accepted: 3 November 2021
Published: 8 November 2021

Publisher's Note: MDPI stays neutral with regard to jurisdictional claims in published maps and institutional affiliations.



Copyright: © 2021 by the authors. Licensee MDPI, Basel, Switzerland. This article is an open access article distributed under the terms and conditions of the Creative Commons Attribution (CC BY) license (<https://creativecommons.org/licenses/by/4.0/>).

Abstract: We describe a potentially new species of a platinum cupride–stannide mineral (PCSM) of composition Pt(Cu_{0.67}Sn_{0.33}). It occurs in a placer deposit in the River Bolshoy Khailyk, southern Krasnoyarskiy kray, Russia. A synthetic equivalent of PCSM was obtained and characterized. The PCSM occurs as anhedral or subhedral grains up to 15 μm × 30 μm in association with various platinum-group minerals, Rh–Co-rich pentlandite and magnetite, all hosted by a placer grain of Cu–Au–Pt alloy. Synchrotron micro-Laue diffraction studies indicate that the PCSM mineral is tetragonal and belongs to the inferred space-group *P4/mmm* (#123). Its unit-cell parameters are *a* = 2.838 (3) Å, *c* = 3.650 (4) Å, and *V* = 29.40 (10) Å³, and *Z* = 1. The *c/a* ratio calculated from the unit-cell parameters is 1.286. These characteristics are in good agreement with those obtained for specimens of synthetic Pt(Cu_{0.67}Sn_{0.33}). A review on related minerals and unnamed phases is provided to outline compositional variations and extents of solid solutions in the relevant systems PtNi–PtFe–PtCu, PdCu–PdHg–PdAu, PdHg–PtHg, and AuCu–PtCu. The PCSM-bearing mineralization appears to be related genetically with an ophiolitic source-rock of the Aktovraskiy complex of the western Sayans. The unnamed phase likely crystallized from microvolumes of a highly fractionated melt rich in Cu and Sn.

Keywords: ternary Pt–Cu–Sn phase; intermetallic compounds and alloys; platinum-group minerals; PGE–Cu–Au mineralization; ophiolite complexes; placer deposits; Bolshoy Khailyk; western Sayans; Russia

1. Introduction

The placer deposits of the River Bolshoy Khailyk, western Sayans, in the Ermakovskiy district, southern Krasnoyarskiy kray of Russia [1] are known for assemblages of platinum-group minerals (PGM) and associated PGE–Au phases. The river drains the Aktovraskiy ophiolitic complex, part of the Kurtushibinskiy belt. Bodies of serpentinite are fairly abundant in the drainage area. We focus here on a potentially new species of a platinum cupride–stannide mineral (PCSM) of composition Pt(Cu_{0.67}Sn_{0.33}); we describe its properties and characteristics. This mineral is closely related to synthetic Pt(Cu_{0.67}Sn_{0.33}), a phase recognized recently in the ternary system Pt–Cu–Sn [2]. Tatyanaite, Pt₉Cu₃Sn₄, is another

compound in that system [3]. As a second objective, we provide a comprehensive review of structurally related alloys and intermetallic compounds in the systems PtNi–PtFe–PtCu, PdCu–PdHg–PdAu, PdHg–PtHg, and AuCu–PtCu. These include tetraferroplatinum, PtFe, and tulameenite, Pt₂CuFe [4,5], both important sources of Pt in various parageneses of Pt–Fe alloy minerals, e.g., [6]. We explore how these minerals and phases can be grouped on the basis of the degree of order of constituent metals in the relevant structures.

2. Materials and Methods

Our materials involve natural specimens of PCSM as well as the synthetic equivalent in terms of compositional and structural characteristics. Compositions of the mineral were investigated with wavelength-dispersive analysis (WDS) using a Camebax-micro electron microprobe (Cameca Inc. Gennevilliers, France) at the Sobolev Institute of Geology and Mineralogy, Russian Academy of Sciences, Novosibirsk, Russia, operated at 20 kV and 20 nA, with a beam diameter of ~1 µm. The following X-ray lines were used: PtLα, PdLα, SnLα, CuKα, NiKα, FeKα, and AuMα. Pure platinum, pure palladium, pure gold, synthetic FeNiCo, CuFeS₂, and SnO₂ were used as standards. The estimated values of minimum-detection levels (MDL) are ≤0.1 wt.%.

Quantitative analyses of the synthetic PCSM were conducted at the R&D center of Norilsk Nickel at the Institute of Mining, Geology and Geotechnology of the Siberian Federal University, Krasnoyarsk, by means of scanning electron microscopy and energy-dispersive analysis (SEM–EDS) done on a Tescan Vega III SBH system (Tescan Orsay Holding, Brno, Czech Republic) equipped with an Oxford X-Act spectrometer (Oxford Instruments Nanoanalysis, Wycombe, UK). The operating conditions were held at an accelerating voltage of 20 kV and a beam current of 1.2 nA. The following X-ray lines (and standards) were used: the K line for Cu (synthetic chalcopyrite), the L line for Sn (pure Sn), and Pt (pure Pt).

Reflectance measurements of the synthetic PCSM specimen were performed using a LomoMSFU-KYu-30.54.072 microspectrophotometer (OOO “Lomo”, St. Petersburg, Russia), using a single-crystal silicon standard (KEF 4.5/0.3) provided by the S.I. Vavilov State Optical Institute, an All-Russian Research Center in St. Petersburg, Russia. The micro-indentation values of hardness were measured using a PMT–3 equipment (OOO “Lomo”, St. Petersburg, Russia), also on the synthetic analogue.

Synchrotron micro-Laue diffraction studies of the natural specimen of PCSM were carried out at beam line 12.3.2 of the Advanced Light Source (ALS), Berkeley, California, USA. The Laue diffraction patterns were collected using a PILATUS 1M area detector operated in reflection geometry. The patterns were indexed and analyzed using XMAS v.6 [7]. A monochromator energy scan was performed to determine the lattice parameters.

Single-crystal electron-backscatter diffraction (EBSD) analyses were performed on the natural specimen of PCSM using an HKL EBSD system (Oxford Instruments, High Wycombe, United Kingdom) on a ZEISS 1550VP Field-Emission SEM (Carl Zeiss Microscopy Deutschland GmbH, Oberkochen, Germany) operated at 20 kV and 6 nA in focused-beam mode, with a 70° tilted stage and in a variable pressure mode (25 Pa). The focused electron beam is several nanometers in diameter. The spatial resolution for diffracted backscatter electrons is ~30 nm. The EBSD system was calibrated using a single-crystal silicon standard.

X-ray diffraction patterns of synthetic Pt(Cu_{0.67}Sn_{0.33}) were collected at ambient temperature with a Panalytical X'Pert diffractometer (Malvern Panalytical Ltd., Malvern, United Kingdom) used with CuKα₁ radiation from a Cu anode operating at 40 kV and 30 mA; a focusing Johansson Ge monochromator was used. The patterns were measured with a PIXcel3D 2 × 2 detector. The indexing was performed using the DICVOL program [8]; Le Bail and Rietveld refinements were performed using the program FULLPROF [9]. A linear interpolation of approximately 30 manually selected points for the background and a pseudo-Voigt profile function were used.

3. Results and Observations

3.1. Occurrence and Associated Minerals

The potentially new platinum cupride–stannide mineral was found in a placer deposit located at a remote locality (*ca.* N 51°51′19.51″, E 92°33′42.82″) along River Bolshoy Khailyk [1]. Osmium-, Ir-, and Ru-dominant alloys (i.e., the minerals osmium, iridium, and ruthenium, respectively) are the main PGM in the Bolshoy Khailyk placer. Isoferroplatinum-type Pt–Fe alloys are subordinate, whereas alloy grains of the series (Pt,Ir)(Ni,Fe,Cu)_{3–x}–(Ir,Pt)(Ni,Fe,Cu)_{3–x} are uncommon.

Inclusions in the PGE alloy minerals include clinopyroxene, i.e., diopside: Wo_{48.3–48.6}En_{48.4–48.5}Fs_{2.6}Aeg_{0.4–0.7}; Mg# 96.9–97.9, chromian spinel, i.e., magnesiochromite: Mg# up to 71, and serpentine, which all are highly magnesian, consistent with a primitive ultrabasic source-rock. The amphibole inclusions correspond to actinolite, magnesio-hornblende and barroisite. Along with cobaltian pentlandite and magnetite, PCSM forms small domains up to 15 μm × 30 μm in size, typically irregular in shape (Figure 1); these are hosted by a placer grain of Cu–Au–Pt alloy ~1 mm across. In addition, the host grain contains inclusions of members of the tulameenite–ferronickelplatinum series and a member of the tolovkite–irarsite–hollingworthite solid solution.

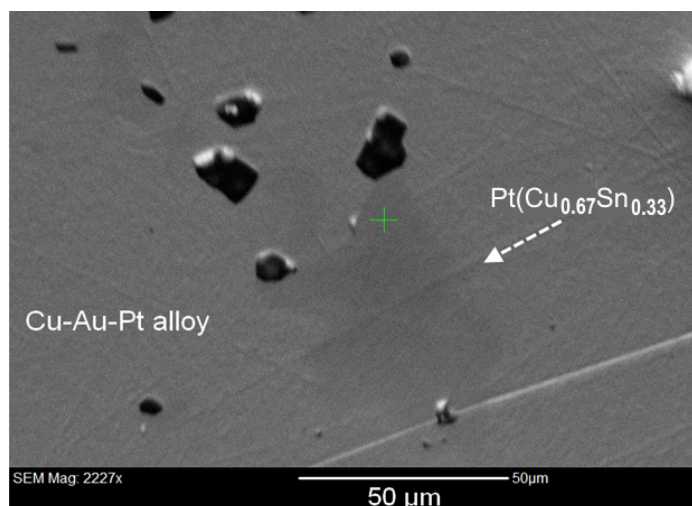


Figure 1. One of five domains of Pt(Cu_{0.67}Sn_{0.33}) encountered in a placer grain of Cu–Au–Pt alloy from the Bolshoy Khailyk placer. It is slightly darker than its host. The location of the EBSD spot is marked with a green cross symbol.

The sulfide species observed in the placer are members of the laurite–erlichmanite series, cooperite, bowieite (Cu-rich), a monosulfide-type phase, (Fe_{0.40}Ni_{0.39}Cu_{0.19})Σ_{0.98}S_{1.02}, a bornite-like phase, (Cu_{4.06}Fe_{1.47})Σ_{5.53}S_{4.5}, and a godlevskite-like phase, Ni_{9.5}S_{7.5}. Less common and rare minerals include sperrylite, a zoned oxide Ru₆Fe³⁺₂O₁₅, and an uncommon variety of seleniferous and rhodiferous sperrylite (Pt,Rh)(As,Se,S)₂ [1,10].

3.2. PCSM: Appearance, Physical, and Optical Properties

Grains of PCSM are opaque, with a metallic luster. It is metallic. The micro-indentation values of hardness measured on the synthetic analogue are in the range 94.8–100.8 kg/mm², which corresponds to a Mohs hardness of ~2½. Cleavage, parting, and fractures were not observed. The density could not be measured owing to the small grain size. The calculated density, 14.75 (5) g·cm^{−3}, is based on the empirical formula and unit-cell volume refined from the synchrotron microdiffraction data.

In reflected light, the color is yellowish cream; bireflectance, pleochroism, and internal reflections were not observed. The mineral is weakly anisotropic. The reflectance values obtained in air for the synthetic analogue, (Pt_{0.97}Cu_{0.03})Σ_{1.00}(Cu_{0.67}Sn_{0.33})Σ_{1.00}, are presented in Table 1 and Figure 2.

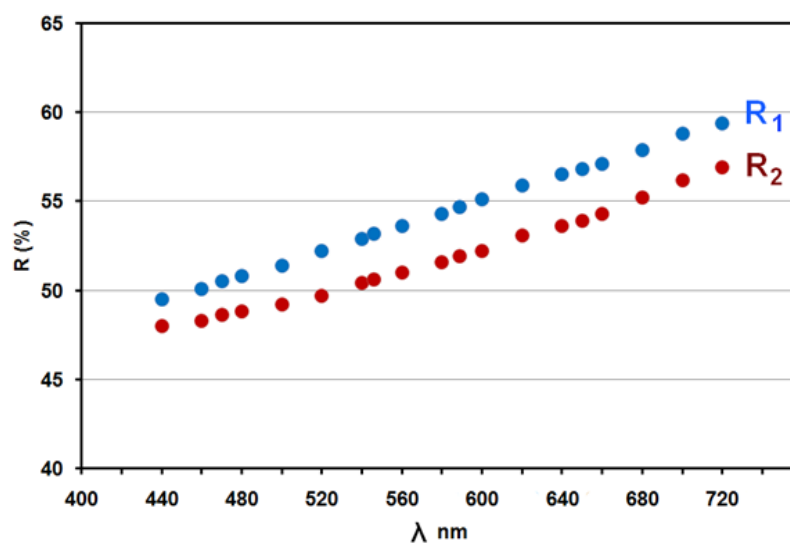


Figure 2. Reflectance spectra for synthetic $\text{Pt}(\text{Cu}_{0.67}\text{Sn}_{0.33})$, measured in air.

Table 1. Reflectance values of synthetic $\text{Pt}(\text{Cu}_{0.67}\text{Sn}_{0.33})$ measured in air.

λ (nm)	R_1 (%)	R_2 (%)	λ (nm)	R_1 (%)	R_2 (%)
440	49.5	48.0	589 (COM)	54.7	51.9
460	50.1	48.3	600	55.1	52.2
470 (COM)	50.5	48.6	620	55.9	53.1
480	50.8	48.8	640	56.5	53.6
500	51.4	49.2	650 (COM)	56.8	53.9
520	52.2	49.7	660	57.1	54.3
540	52.9	50.4	680	57.9	55.2
546 (COM)	53.2	50.6	700	58.8	56.2
560	53.6	51.0	720	59.4	56.9
580	54.3	51.6			

Note. These values pertain to synthetic $(\text{Pt}_{0.97}\text{Cu}_{0.03})_{\Sigma 1.00}(\text{Cu}_{0.67}\text{Sn}_{0.33})_{\Sigma 1.00}$, measured on a representative specimen. COM: wavelengths recommended by the Commission on Ore Mineralogy, IMA.

3.3. Compositional Data

Electron-microprobe analysis (Table 2) of the mineral yields the formula $(\text{Pt}_{0.80}\text{Pd}_{0.17}\text{Au}_{0.02})_{\Sigma 0.99}(\text{Cu}_{0.61}\text{Sn}_{0.34}\text{Fe}_{0.05}\text{Ni}_{0.02})_{\Sigma 1.02}$, calculated on the basis of a total of 2 a.p.f.u. (atoms per formula unit). An alternative formula, $(\text{Pt,Pd})_3\text{Cu}_2\text{Sn}$, with a distinct site for Sn, is not confirmed by structural results. The formula $\text{Pt}(\text{Cu}_{0.67}\text{Sn}_{0.33})$ requires Pt 70.47, Cu 15.38, and Sn 14.15, total 100 wt.%. Tin is an essential constituent, but Pd is not. On the basis of the inferred composition, a synthetic equivalent of the PCSM was successfully obtained and characterized by [2].

Table 2. Composition of unnamed $\text{Pt}(\text{Cu}_{0.67}\text{Sn}_{0.33})$ from the Bolshoy Khailyk placer, western Sayans, Russia.

Constituent	Mean (wt.%)	Range (wt.%)
Pt	59.90	57.17–64.22
Pd	6.92	3.28–8.30
Cu	14.71	14.49–14.94
Sn	15.33	14.19–16.14
Au	1.47	0.55–2.67
Fe	1.01	0.82–1.32
Ni	0.36	0.31–0.43
Total	99.70	98.80–100.39

Note. Results of a total of five data points ($n = 5$), listed in weight %, that were acquired by means of WDS analysis.

3.4. Characterization of the Synthetic Analogue

The synthetic analogue Pt(Cu_{0.67}Sn_{0.33}) was obtained [2] by heating stoichiometric mixtures of analytical grade powders of platinum (ChemPUR 99.95%), copper (ChemPUR 99.99%), and tin (MERCK 99%) in a molar proportion 3:2:1 (as inferred from Pt:Cu:Sn = 3:2:1 in the specimens from Bolshoy Khailyk). The mixtures were homogenized in an agate mortar and pressed into pellets. On the basis of differential scanning calorimetry (DSC) measurements, a heating rate of 6 K/min was selected for all syntheses. In one set of experiments, the furnace was switched off after holding the charge at the maximum temperature, and the pellets were cooled down. In a second set of experiments, the pellets were quenched to ambient temperature in less than one minute using compressed air. A total of 12 analyses (quantitative SEM/EDS) of different portions of the synthetic phase gave the following mean (and ranges): Pt 70.01 (69.2–70.8), Cu 16.35 (16.0–16.6), and Sn 14.53 (14.0–14.9), for a total of 100.9 wt.%, corresponding to (Pt_{0.97}Cu_{0.03})_{Σ1.0}(Cu_{0.67}Sn_{0.33})_{Σ1.0} (on the basis of Σatoms = 2 a.p.f.u.).

In addition, the phase Pt(Cu_{0.67}Sn_{0.33}) was synthesized in an arc-melter (MAM-1, E. Bühler, GmbH, Hechingen) by melting the mixture of elements. Temperatures in the arc melter were above 2000 K. After the synthesis, the pellet rapidly reached ambient temperature [2].

3.5. Crystallography and Crystal Structure

The grains of PCSM are polycrystalline, as are those of the synthetic phase. Our attempts to extract a single crystal were unsuccessful, and even ~15 micrometer-sized fragments turned out to be polycrystalline. Thus, a single-crystal study could not be carried out.

The X-ray diffraction pattern of PCSM is reported in Table 3. The mineral is tetragonal, and the inferred space group is *P4/mmm* (#123). The unit-cell parameters are *a* = 2.838(3) Å, *c* = 3.650(4) Å, *V* = 29.40(10) Å³, and *Z* = 1. The *c*:*a* ratio calculated from the unit-cell parameters is 1.286.

Table 3. X-ray powder-diffraction data (*d* in Å) for unnamed Pt(Cu_{0.67}Sn_{0.33}) from the Bolshoy Khailyk placer, western Sayans, Russia.

<i>d</i> _{obs.}	<i>d</i> _{calc.}	<i>I</i> _{meas.}	<i>I</i> _{calc.}	<i>h</i>	<i>k</i>	<i>l</i>	<i>d</i> _{obs.}	<i>d</i> _{calc.}	<i>I</i> _{meas.}	<i>I</i> _{calc.}	<i>h</i>	<i>k</i>	<i>l</i>
3.6500	3.6364	13.0	11.6	0	0	1	0.9236	0.9195	1.1	1.0	2	0	3
2.8380	2.8221	14.2	12.6	1	0	0	0.9157	0.9107	5.5	5.5	3	0	1
2.2405	2.2295	100.0	100.0	1	0	1	0.9125	0.9091	1.4	1.4	0	0	4
2.0068	1.9955	36.4	36.3	1	1	0	0.8975	0.8924	5.2	5.2	3	1	0
1.8250	1.8182	13.7	13.7	0	0	2	0.8793	0.8747	4.9	5.0	2	2	2
1.7585	1.7494	7.9	7.0	1	1	1	0.8783	0.8742	9.9	9.9	2	1	3
1.5350	1.5285	5.3	4.8	1	0	2	0.8715	0.8667	2.0	1.8	3	1	1
1.4190	1.4111	12.2	12.1	2	0	0	0.8687	0.8653	1.0	0.9	1	0	4
1.3502	1.3440	20.5	20.5	1	1	2	0.8399	0.8355	1.0	0.9	3	0	2
1.3226	1.3155	3.4	3.0	2	0	1	0.8307	0.8273	4.4	4.4	1	1	4
1.2692	1.2621	3.0	2.6	2	1	0	0.8054	0.8011	8.5	8.5	3	1	2
1.2167	1.2121	0.6	0.6	0	0	3	0.7871	0.7827	0.9	0.8	3	2	0
1.1988	1.1923	27.0	26.9	2	1	1	0.7741	0.7704	0.9	0.8	2	2	3
1.1202	1.1147	10.6	10.6	2	0	2	0.7694	0.7652	8.2	8.3	3	2	1
1.1182	1.1138	10.6	10.5	1	0	3	0.7675	0.7642	4.1	4.2	2	0	4
1.0420	1.0368	3.2	2.9	2	1	2	0.7468	0.7432	4.1	4.2	3	0	3
1.0404	1.0360	1.6	1.4	1	1	3	0.7409	0.7377	1.8	1.7	2	1	4
1.0034	0.9978	3.6	3.6	2	2	0	0.7300	0.7273	0.2	0.2	0	0	5
0.9675	0.9622	1.3	1.2	2	2	1	0.7228	0.7189	1.9	1.8	3	2	2
0.9460	0.9407	0.6	0.6	3	0	0	0.7222	0.7187	1.9	1.8	3	1	3

Note. Results of synchrotron micro-Laue diffraction studies were indexed and analyzed using the software package XMAS v.6 [6]. The calculated values were obtained for the synthetic counterpart.

The EBSD patterns of the PCSM (Figure 3a–d) are indexed satisfactorily on the basis of the $P4/mmm$ structure obtained via micro-Laue synchrotron diffraction, with a mean angular deviation of 0.38° – 0.45° .

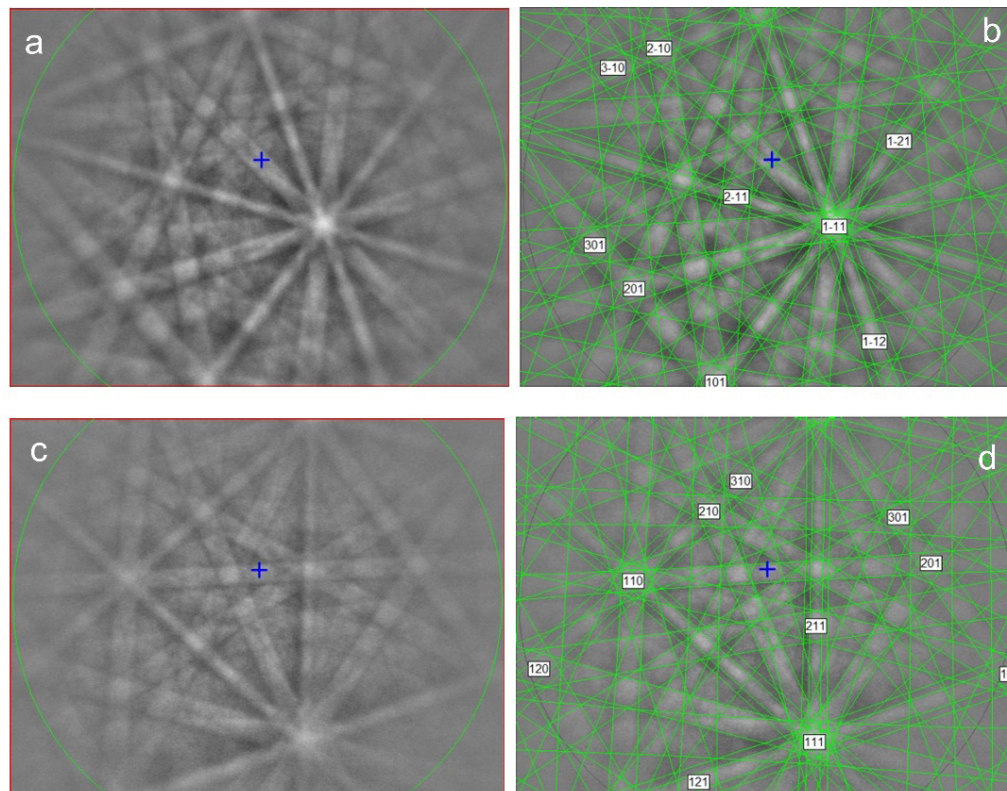


Figure 3. EBSD patterns (a,c) of two grains of the $\text{Pt}(\text{Cu}_{0.67}\text{Sn}_{0.33})$ mineral with different orientations, and (b,d) these patterns indexed with the $P4/mmm$ structure.

The structure of synthetic $\text{Pt}(\text{Cu}_{0.67}\text{Sn}_{0.33})$ was determined on the basis of powder-diffraction data [2]. The observed lattice parameters, the crystal structure, and the reliability factors are presented in Tables 4 and 5. Refinements of the site occupancies gave $\text{Pt}(\text{Cu}_{0.59(5)}\text{Sn}_{0.41(5)})$ as an approximate composition, which is in fairly good agreement with the $\text{Pt}(\text{Cu}_{0.67}\text{Sn}_{0.33})$ composition of the natural specimen. The crystal structure of the PCSM is shown in Figure 4. It is a tetragonal CuAu-type or $L1_0$ -type structure, in which Pt occupies the Wyckoff position $1a$ (0,0,0) and disordered Cu and Sn occupy the Wyckoff position $1d$ ($\frac{1}{2}, \frac{1}{2}, \frac{1}{2}$) in the space group $P4/mmm$ (as obtained from the refined site-occupancy via Rietveld refinement of the synthetic analogue $\text{Pt}(\text{Cu}_{0.67}\text{Sn}_{0.33})$) [2].

The cell parameters of the synthetic analogue of the PCSM are $a = 2.82205(1) \text{ \AA}$, $c = 3.63637(2) \text{ \AA}$, and $V = 28.9599(2) \text{ \AA}^3$; the space group is $P4/mmm$ (Tables 4 and 5) [2]. These values are close to the parameters obtained for the PCSM specimen from Bolshoy Khailyk.

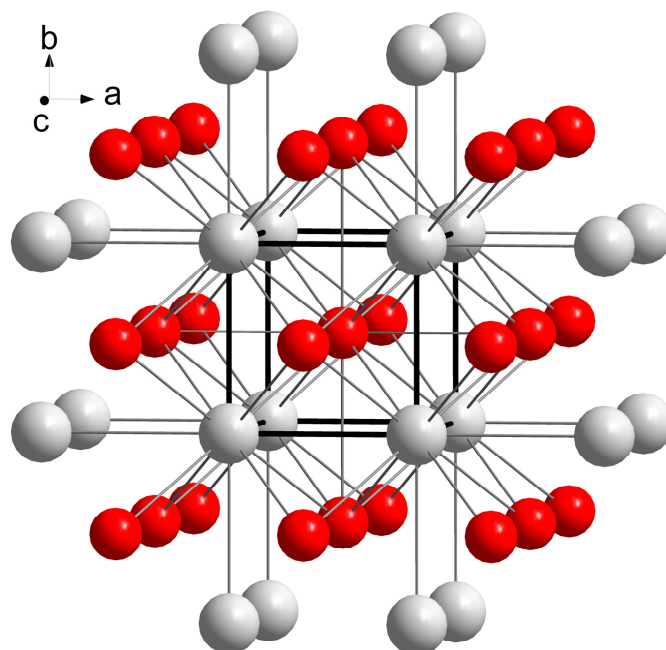


Figure 4. The crystal structure of the $\text{Pt}(\text{Cu}_{0.67}\text{Sn}_{0.33})$ compound along the ab plane. Atoms of Pt are shown by the gray spheres, and Cu, Sn are the red spheres.

Table 4. Lattice parameters of synthetic $\text{Pt}(\text{Cu}_{0.67}\text{Sn}_{0.33})$ from Rietveld refinement and from density functional theory (DFT) calculations *.

Lattice Parameters ^[a]	S4	S5	DFT ^[b]
a (Å)	2.82205(1)	2.82101(3)	2.8762
c (Å)	3.63637(2)	3.64874(6)	3.6984
V (Å ³)	28.960(1)	29.037(1)	30.56

^[a] Density = 15.976 g/cm³, from X-ray diffraction. ^[b] The DFT values are $1/3$ of the supercell used in all the calculations. The angles of the supercell deviated by $<0.1^\circ$ from 90° after the optimization of the geometry. * After Juarez-Arellano et al., 2020 [2]. Syntheses S4 and S5 involved a first step at 523 K for five hours and a second step at 1023 K for 10 h.

Table 5. Crystal structure of synthetic $\text{Pt}(\text{Cu}_{0.67}\text{Sn}_{0.33})$ on the basis of results of Rietveld refinement and reliability factors *.

	Atom	Wyckoff Position	x/a	y/b	z/c	B (Å ²)	Occupancy
S4	Pt	1a	0	0	0	0.10(2)	1.0
	Cu, Sn	1d	0.5	0.5	0.5	0.29(3)	0.638(3), 0.362(3)
S5	Pt	1a	0	0	0	0.22(6)	1.0
	Cu, Sn	1d	0.5	0.5	0.5	1.01(9)	0.544(12), 0.456(12)
	χ^2	Rp	R_{wp}	R_{exp}	Rf	data points	independent parameters
S4	4.64	7.91	11.9	5.53	3.06	13,708	14
S5	11.9	9.58	13.6	3.95	8.93	6855	14

* After Juarez-Arellano et al., 2020 [2]. Products of synthesis S4 and S5 are as defined in Table 4.

4. Discussion

4.1. Genetic Implications

The PCSM grains are hosted by a composite grain of (Au,Pt)Cu alloy recovered in a remote placer deposit along the Bolshoy Khailyk river. Previously, a similar grain of (Au,Pt)Cu alloy was reported from a placer along River Zolotaya in the same area [11]. Similar grains of the (Au,Pt)Cu alloy have been documented at other localities: the Tulameen complex, Canada [12], the Sotajarvi area, Finland [13] and, in situ, in the Kondyor complex, Russian Far East [14]. As noted, the detrital grain hosting the PCSM grains also hosts

several grains of various PGM, Co-(Rh)-rich pentlandite, and Cr–Mg–Mn-rich magnetite, among others. The observed system thus involves at least 17 elements (Cu, Au, Pt, Rh, Pd, Ir, Fe, Co, Ni, S, Sb, As, Sn, O, Cr, Mn, Mg), which occur, as major or minor constituents, in minerals of the PCSM-bearing grain. The large variety of participating elements clearly points to a natural origin of this specimen.

The Aktovraskiy ophiolitic complex is considered to represent the lode source for the PCSM-bearing association. The notable extent of Ru enrichment in the associated Os–Ir–Ru alloy minerals is consistent with an ophiolitic source [1]. The PCSM-bearing assemblages presumably formed after the crystallization of chromian spinel (magnesiocromite) and Fe-enriched olivine. During the crystallization of the Os–Ir–Ru alloy phases, a local buildup of the incompatible Cu + Au, along with subordinate Pt, likely led to the crystallization of PCSM from globules of remaining melt.

4.2. Compositional Variations and Solid Solutions in Related Minerals and Compounds

Members of a potentially large family of natural alloys and intermetallic compounds, mostly isotypic with AuCu(I) [15], are related to mineral PCSM and like it, crystallize in space group $P4/mmm$. They include (1) natural solid-solutions pertaining to the system PtNi–PtFe–PtCu and the synthetic analogues of PtFe and PtNi (e.g., [4,5,16–18]); (2) potarite, PdHg, and its synthetic equivalent [19–22], as well as an auriferous variety of potarite, Pd(Hg,Au) [23]; and (3) tetra-auricupride, AuCu ([24], cf. [18]) and its variants having platiniferous compositions: (Au,Pt)Cu, e.g., [10].

Mineral PCSM corresponds to the Cu-dominant analogue of tetraferroplatinum (PtFe; $a = 2.7235(10)$, $c = 3.720(3)$ Å: IMA1974-012b: [4,5,25]); it consists of disordered metals in the ‘tP2’ structure of space group $P4/mmm$. It is also related to tulameenite (Pt₂FeCu; $a = 3.891(2)$, $c = 3.577(2)$ Å: IMA1972-016: [4]) and ferronickelplatinum (Pt₂FeNi; $a = 3.871$, $c = 3.635$ Å: IMA1982-071: Rudashevsky et al., 1983 [26]), which exhibit the ‘tP4’ structure with ordered metal atoms in a larger unit cell but the same space group $P4/mmm$ as the ‘tP2’ structure. The “(Cu,Fe)Pt” formula of tulameenite listed by P. Bayliss in [18] is not correct; his proposal is not accepted by the authors of the description of tulameenite (L.J. Cabri, pers. commun.). The type tulameenite displays a Fe:Cu ratio of 1:1, and Cu is not dominant. As tulameenite was not redefined, the proposal of Cabri et al., 1973 [4], including the unit-cell parameters and the Pt₂FeCu formula with a Fe:Cu ratio of about 1:1, is still valid.

Mineral PCSM differs from hongshiite, PtCu [27,28], see also [29], from synthetic PtCu that crystallizes in space group $Fm\bar{3}m$ (with $a = 3.796$ Å: ICDD-00-048-1549 or $a = 3.799$ Å [2]), and from tatyanaite (Pt,Pd)₉Cu₃Sn₄, which is orthorhombic [3].

4.3. Solid Solutions in the Ternary System PtNi–PtFe–PtCu

Natural series of solid solutions pertaining to this system were examined on the basis of 510 data points collected in the literature (Table 6; Figures 5 and 6). Nine sets of compositional data were evaluated, which are judged to be representative of various complexes located in different geological settings worldwide, including the Alaskan–Uralian–(Aldan)-type complexes (sets 1–3), layered intrusions (set 4), ophiolite-related deposits (set 5), an uncategorized chromitite (set 6), massive sulfide Cu–Ni ores (set 7), Ti-rich mineralization developed in alkaline ultramafic complexes (set 8), and different suites of placer deposits (set 9).

Table 6. Worldwide occurrences and reviewed sets of compositions of solid solutions belonging to the system PtNi–PtFe–PtCu.

	Type	Localities and Occurrences	References
Set #1 (<i>n</i> = 33)	Alaskan-Uralian-type complexes and related placers in northern America	Tulameen complex and placers in R. Tulameen and R. Similkameen areas, British Columbia, Canada. Salmon river placer deposit, Goodnews Bay, Alaska, USA.	Cabri et al., 1973, 1996 [3,30] Nixon et al., 1990 [17] Tolstykh et al., 2002 [31]
Set #2 (<i>n</i> = 256)	Uralian-Alaskan-type clinopyroxenite-dunite and related complexes and derived placers, Ural Platinum Belt, Urals, Russia	Nizhny Tagil; Kachkanar; Svetly Bor (Svetloborsky); Kamenushinsky; Veresoborsky; Solovyova Gora; Kytlym; Iovskiy; Uktus (chromitites and Chr-rich zones); Nevyansk and Kushvinskiy placers.	Cabri and Genkin, 1991 [32] Cabri et al., 1996 [30] Garuti et al., 2002, 2003 [33,34] Augé et al., 2005 [35] Tolstykh et al., 2011, 2015 [36,37] Volchenko, 2011 [38] Zaccarini et al., 2013 [39] Barannikov and Osovetskiy, 2014 [40] Stepanov, 2015 [41] Malitch and Badanina, 2015 [42] Palamarchuk et al., 2017 [43]
Set #3 (<i>n</i> = 98)	Alaskan-Uralian (Aldan)-type and related complexes (and associated placers) in Russian Far East and Polar Siberia	Gal'moenan (Koryak region); Mount Filippa and R. Pustaya placer (Kamchatka); Kondyor (northern Khabarovskiy kray); Guli (Maymecha-Katui region, Polar Siberia).	Tolstykh et al., 2000 [44] Malitch and Thalhammer, 2002 [45] Sidorov et al., 2004, 2012 [46,47]
Set #4 (<i>n</i> = 37)	Layered intrusions and associated deposits	Onverwacht and Mooihoek pipes; LG and MG chromitites; detrital occurrences, Bushveld complex, South Africa. Great Dyke, Zimbabwe (detrital grains). Zones of sulfide mineralization in Lukkulaivaara and Burakovskiy intrusions, Karelia, Russia. Sisim Placer Zone (Lysanskiy layered complex), Eastern Sayans, Russia.	Cabri and Feather, 1975 [4] Cabri et al., 1977 [25] Yakovlev et al., 1991 [48] Rudashevskiy et al., 1992 [49] Barkov and Lednev, 1993 [50] Grokhovskaya et al., 2005 [51] Melcher et al., 2005 [52] Oberthür et al., 2013, 2016 [53,54] Barkov et al., 2018 [55]
Set #5 (<i>n</i> = 27)	Ophiolite-related deposits	R. Northern Pekul'ney, Pekul'ney Ridge, Chukotskiy (Chukotka) Autonomous Okrug, northeastern Russia; Olkhovaya-1 placers (Karaginsky ophiolite complex), Kamchatka, Russia. Placer of R. Bolshoy Khailyk, western Sayans, Russia.	Rudashevskiy et al., 1983 [26] Tolstykh et al., 2009 [56] Barkov et al., 2018 [9]
Set #6 (<i>n</i> = 3)	Other chromitite deposits in ultramafic rocks	Soldzherskiy Ultrabasic-basic complex of Tuva (Tyva), southern Siberia, Russia.	Agafonov et al., 1993 [57]
Set #7 (<i>n</i> = 2)	Massive sulfide deposits	Massive talnakhite ore, Noril'sk orefield (northern Krasnoyarskiy kray, Russia).	Cook et al., 2002 [58]
Set #8 (<i>n</i> = 7)	Ti-rich oxide mineralization in Alkaline Ultramafic complexes	Lesnaya Varaka complex; Por'yerechenskiy deposit, Kola Peninsula, Russia.	Barkov et al., 1998 [59] Neradovskiy et al., 2017 [60]
Set #9 (<i>n</i> = 47)	Various placer deposits	Rio Condoto, Choco, Colombia; Chindwin River area, Burma; Joubdo (Yubdo), Ethiopia; Placers in British Columbia, Canada.	Cabri et al., 1996 [30] Laflamme, 2002 [61] Barkov et al., 2005, 2008 [62,63]

Note. A total of 510 data points (*n* = 510), collected in these sets, are evaluated in Figures 5 and 6.

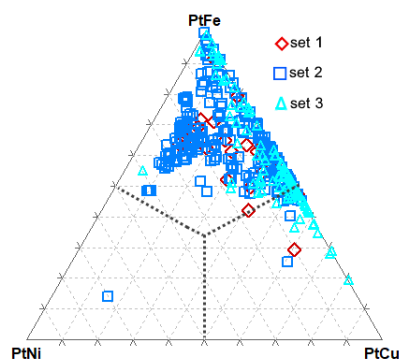


Figure 5. Compositional variations of alloy minerals from various complexes and deposits, shown in PtNi–PtFe–PtCu compositional space (molar proportions are based on nine sets of data points provided in the sources listed in Table 6).

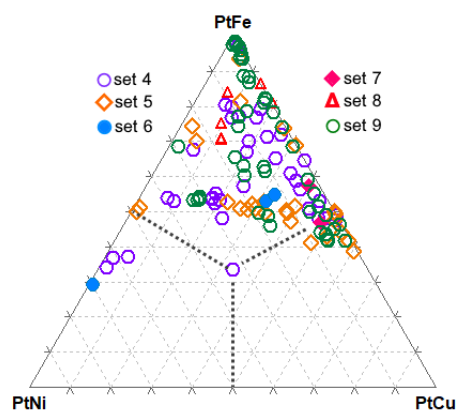


Figure 6. Compositional variations of alloy minerals from various complexes and deposits, shown in PtNi–PtFe–PtCu compositional space (molar proportions are based on nine sets of data points provided in the sources listed in Table 6).

Values Pt + PGE and $\Sigma(\text{Fe} + \text{Cu} + \text{Ni} + \text{Sb} + \text{Hg})$ are in the ranges 0.7–1.2 and 0.8–1.3 a.p.f.u. for $\Sigma\text{atoms} = 2$ a.p.f.u., respectively. The mean composition is notably stoichiometric, yielding the 1:1 proportion calculated for $n = 510$ data points. The observed variations imply that the excess atoms could enter both the Pt and base-metal sites.

The Alaskan–Uralian–(Aldan)-type complexes are most important sources of these alloy minerals (Figures 5 and 6). The major trend extends along the PtFe–PtCu join; numerous compositions are Cu-dominant. In contrast, the PtFe–PtNi series is much more limited, with relatively few alloy samples having a Ni-dominant compositions (#1, 12, 13, Table 7), reported from the Soldzhersky complex, Tuva, Russia, the Bushveld layered complex, South Africa, and from the Butyrinskoye deposit, Kytlym complex, Urals, Russia [38,52,57]. Interestingly, the PtNi–PtFe join is totally free of data points in spite of a large number of compositions examined from these complexes (Figure 5). Thus, the Cu-for-Fe type of substitution is more common, whereas the Ni-for-Fe scheme likely requires special conditions of crystallization.

The maximum extent of Cu enrichment occurs in the phase $\text{Pt}_{1.10}(\text{Cu}_{0.65}\text{Fe}_{0.26})_{\Sigma 0.91}$ analyzed in the River Pustaya placer, Kamchatka, Russia [44]. The same level of Cu is attained in the unnamed $\text{Pt}(\text{Cu}_{0.67}\text{Sn}_{0.33})$ at Bolshoy Khailyk.

A pure “PtCu” component is not an end member in these series. As noted, it corresponds to hongshiite, PtCu, which is trigonal (space group: $R\bar{3}2$, $R\bar{3}m$, or $R\bar{3}m$), with the unit-cell parameters: $a = 10.713 \text{ \AA}$, $c = 13.192 \text{ \AA}$, and $Z = 48$ [28], and to synthetic PtCu of trigonal structure [29]. Synthetic PtCu is also known to crystallize in space group $Fm\bar{3}m$ (with $a = 3.796 \text{ \AA}$: ICDD-00-048-1549 or $a = 3.799 \text{ \AA}$ [2]). Thus, the presence of Sn, Cu, Sb, or Hg, or other components is, indeed, significant to stabilize the $P4/mmm$ structure of the mineral PCSM.

4.4. Solid Solutions in the Ternary System PtNi–PtFe–PtCu

Elevated amounts of Pd and Ir are typical of PtFe alloys (Figures 7 and 8), as they are in other species of Pt–Fe minerals, i.e., Fe-bearing platinum and isoferroplatinum, cf. [6]. Levels of Pd attain 0.3 Pd a.p.f.u. (#1, 4 in Table 7) [38,55]. A value greater than 0.35 Ir a.p.f.u. (Figure 8), if it corresponds to a single phase, may imply the existence of an Ir-dominant member in this series. Examples of other members of the ternary system are poorer in Ir (Table 7).

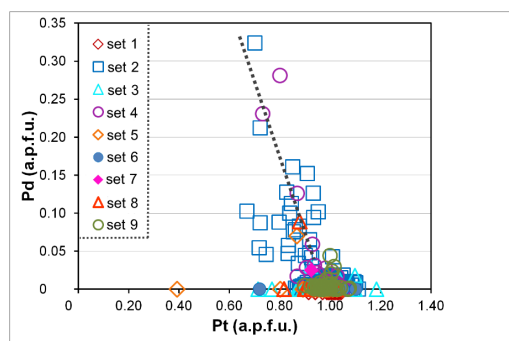


Figure 7. A plot of Pt versus Pd in alloy minerals from various complexes and deposits, on the basis of the literature sources quoted in Table 6 and expressed in terms of atoms per formula unit.

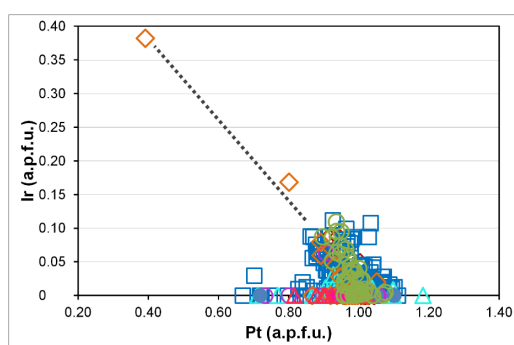


Figure 8. A plot of Pt versus Ir in alloy minerals from various complexes and deposits, on the basis of the literature sources quoted in Table 6 and expressed in terms of atoms per formula unit.

Table 7. Selected examples of compositions of alloy minerals belonging to the system PtNi–PtFe–PtCu.

#.	Locality	Formulae	Comments	References
1	Butyrinskoye deposit, Kytlym complex, Urals, Russia	$(Pt_{0.70}Pd_{0.32}Ir_{0.03})\Sigma_{1.06}(Ni_{0.57}Cu_{0.13}Hg_{0.13}Fe_{0.11})\Sigma_{0.94}$	Pd-rich Ni-dominant, Hg-bearing	Volchenko, 2011 [38]
2	Kytlym complex, Urals	$(Pt_{0.72}Pd_{0.21})\Sigma_{0.93}(Fe_{0.48}Cu_{0.39}Ni_{0.13}Hg_{0.05})\Sigma_{1.07}$	Pd-rich	Volchenko, 2011 [38]
3	Bushveld complex, South Africa	$(Pt_{0.73}Pd_{0.23})\Sigma_{0.96}(Cu_{0.53}Fe_{0.49}Ni_{0.01})\Sigma_{1.04}$	Pd-rich	Melcher et al., 2005 [52]
4	Sisim placer (Lysanskiy complex), eastern Sayans, Russia	$(Pt_{0.80}Pd_{0.28})\Sigma_{1.08}(Fe_{0.47}Cu_{0.42}Ni_{0.03})\Sigma_{0.92}$	Pd-rich	Barkov et al., 2018 [55]
5	Ural Platinum Belt, Urals, Russia	$(Pt_{0.96}Ir_{0.10}Rh_{0.02})\Sigma_{1.08}(Fe_{0.72}Ni_{0.15}Cu_{0.04})\Sigma_{0.92}$	Ir-bearing	Cabri and Genkin 1991 [32]
6	Nizhniy Tagil complex, Urals, Russia	$(Pt_{0.93}Ir_{0.11}Rh_{0.01})\Sigma_{1.06}(Fe_{0.79}Cu_{0.08}Ni_{0.08})\Sigma_{0.94}$	Ir-bearing	Tolstykh et al., 2015 [37]
7	Ol'khovaya-1 placer (Karaginsky ophiolite complex), Kamchatskiy kray, Russia	$(Pt_{0.80}Ir_{0.17}Rh_{0.01})\Sigma_{0.98}(Fe_{0.72}Ni_{0.24}Cu_{0.06})\Sigma_{1.02}$	Ir-bearing	Tolstykh et al., 2009 [56]
8	Gal'moenan complex, Koryak region, Russia	$Pt_{0.98}(Cu_{0.60}Fe_{0.43})\Sigma_{1.03}$	Cu-dominant	Sidorov et al., 2012 [47]
9	R. Pustaya placer, Kamchatka, Russia	$Pt_{1.10}(Cu_{0.65}Fe_{0.26})\Sigma_{0.91}$	Cu-dominant	Tolstykh et al., 2000 [44]
10	Ol'khovaya-1 placer Kamchatskiy kray, Russia	$(Pt_{0.96}Rh_{0.03}Os_{0.01})\Sigma_{1.00}(Cu_{0.61}Fe_{0.39}Ni_{0.01})\Sigma_{1.01}$	Cu-dominant	Tolstykh et al., 2009 [56]
11	Placer deposit, British Columbia, Canada	$(Pt_{0.96}Rh_{0.01}Os_{0.01})\Sigma_{0.98}(Cu_{0.58}Fe_{0.43}Ni_{0.02})\Sigma_{1.03}$	Cu-dominant	Barkov et al., 2005 [62]
12	Bushveld complex, South Africa	$(Pt_{0.87}Rh_{0.06}Pd_{0.02}Ru_{0.01})\Sigma_{0.96}(Ni_{0.64}Fe_{0.39}Cu_{0.02})\Sigma_{1.04}$	Ni-dominant	Melcher et al., 2005 [52]
13	Soldzherskiy complex, Tuva, southern central Siberia, Russia	$(Pt_{0.72}Rh_{0.03})\Sigma_{0.75}(Ni_{0.87}Fe_{0.37}Cu_{0.01})\Sigma_{1.25}$	Ni-dominant	Agafonov et al., 1993 [57]
14	Tulameen complex, British Columbia, Canada	$(Pt_{0.96}Pd_{0.02})\Sigma_{0.98}(Cu_{0.53}Fe_{0.26}Sb_{0.15}Ni_{0.09})\Sigma_{1.03}$	Sb-bearing, Cu-dominant	Nixon et al., 1990 [17]
15	Butyrinskoye deposit, Urals, Russia	$(Pt_{0.85}Pd_{0.16}Ir_{0.01})\Sigma_{1.03}(Cu_{0.49}Fe_{0.20}Hg_{0.17}Ni_{0.11})\Sigma_{0.97}$	Hg-bearing, Cu-dominant	Volchenko, 2011 [38]

Note. The formulae are based on a total of two atoms per formula unit (a.p.f.u.).

The maximum levels of Sb and Hg (#14, 15, Table 7) are similar: 0.15 and 0.17 a.p.f.u., respectively [17,38]. The incorporation of Hg is unusual for a Pt–Fe alloy mineral, though it is consistent with the compositions of potarite, PdHg, synthetic PtHg or NiHg, also having the AuCu-type structure [64,65].

4.5. The Systems Involving PdCu, PdHg, and PdAu

Potarite, PdHg, is involved in two solid-solution series (Figure 9): the PdHg–PdCu series, which is present in the Kytlym complex, Urals [38,66], and the PdHg–PdAu series, reported in association with Pd–Pt alloys [67] from Córrego Bom Sucesso, Minas Gerais, Brazil [23,68]. Note that pure “PdCu” presumably does not represent the end-member component in those series because it corresponds to skaergaardite, PdCu, a cubic species crystallizing in space group $Pm\bar{3}m$, with $a = 3.0014(2)$ Å [69]. Representative members of the two series are listed in Table 8 (#12–20). Note that a Cu-dominant member (#12), if isostructural with potarite ($P4/mmm$: #15, Table 9), may correspond to a potentially new species, Pd(Cu,Hg).

As noted by Fleet et al. (2002) [23], the auriferous variety of potarite displays a notable deviation from the ideal atomic proportions toward Pd₃Hg₂. A similar departure also is reported for the tulameenite series, members of which can be somewhat nonstoichiometric: (Pt,PGE)_{1+x}(Fe,Cu,Ni)_{1-x}, where $0 < x < 0.1$ [62].

Table 8. Representative compositions of intermetallic compounds in the platiniferous tetra-auricupride and auriferous–(cupriferous or platiniferous) potarite series.

#	Locality	Formulae	Comments	References
1	Tulameen Alaskan-type complex, British Columbia, Canada	(Au _{0.79} Pt _{0.22})Σ1.01Cu _{0.99}	-	Cabri and Laflamme, 1981 [12]
2	Detrital grain, Sotajoki area, Finland	(Au _{0.66} Pt _{0.27} Pd _{0.13})Σ1.06(Cu _{0.89} Fe _{0.03} Ni _{0.03})Σ0.95	Pd-rich	Törnroos and Vuorelainen, 1987 [13]
3	Zolotaya River placer, western Sayans, Russia	(Au _{0.75} Pt _{0.20} Pd _{0.04} Ir _{0.03} Rh _{0.01})Σ1.03Cu _{0.97}	-	Tolstykh et al., 1997 [11]
4	Kondyor concentrically zoned complex, northern Khabarovskiy kray, Russia	(Au _{0.86} Pt _{0.16})Σ1.02Cu _{0.98}	-	Nekrasov et al., 2005 [14]
5	-	(Au _{0.96} Pt _{0.04})Σ1.00Cu _{1.00}	-	-
6	Kondyor PGE placer deposit, Khabarovskiy kray, Russia	(Au _{0.80} Pt _{0.18} Pd _{0.02})Σ1.00(Cu _{1.00} Fe _{0.01})Σ1.01	-	Shcheka et al., 2004 [70]
7	Noril'sk and Talnakh ore fields, Noril'sk complex, Russia	(Au _{0.82} Pt _{0.09} Pd _{0.06} Ag _{0.02})Σ0.99Cu _{1.00}	-	Spiridonov, 2010 [71]
8	-	(Au _{0.80} Pt _{0.16} Pd _{0.03} Ag _{0.01})Σ1.00Cu _{1.00}	-	-
9	-	(Au _{0.81} Pd _{0.18} Pt _{0.01})Σ1.00Cu _{1.00}	Pd-rich	-
10	R. Bolshoy Khailyk placer, western Sayans, Russia	(Au _{0.73} Pt _{0.28})Σ1.01(Cu _{0.96} Fe _{0.03})Σ0.99	-	Barkov et al., 2019 [10]
11	-	(Au _{0.83} Pt _{0.18})Σ1.01Cu _{0.99}	-	-
12	Pegmatite subtype ore, Butyrinskoye (Butyrin) deposit, Kytlym complex, Ural Platinum Belt, Urals	(Pd _{0.73} Pt _{0.07} Ir _{0.01})Σ0.81(Cu _{0.74} Hg _{0.37} Fe _{0.08} Ni _{0.01})Σ1.20	Cu-dominant, Hg-rich	Volchenko, 2011 [38]
13	-	(Pd _{0.76} Ir _{0.08} Pt _{0.04})Σ0.88(Hg _{0.56} Cu _{0.42} Fe _{0.10} Ni _{0.05})Σ1.13	-	-
14	-	Pd _{0.88} (Hg _{0.88} Cu _{0.21} Fe _{0.03})Σ1.12	-	-
15	-	(Pd _{0.82} Pt _{0.10})Σ0.92(Hg _{0.76} Fe _{0.19} Cu _{0.13})Σ1.08	Pt-bearing	-
16	-	(Pd _{0.56} Pt _{0.49} Rh _{0.01})Σ1.06(Hg _{0.54} Cu _{0.23} Fe _{0.13} Ni _{0.03})Σ0.93	Pt-rich	Zaccarini et al., 2011 [66]
17	-	(Pd _{0.62} Pt _{0.30} Rh _{0.01})Σ0.93(Hg _{0.65} Cu _{0.19} Fe _{0.18} Ni _{0.02} Te _{0.01})Σ1.05	Pt-rich	-
18	-	(Pd _{0.81} Pt _{0.14} Rh _{0.01})Σ0.96(Hg _{0.68} Fe _{0.22} Cu _{0.12} Ni _{0.01})Σ1.03	Pt-bearing	-
19	-	(Pd _{0.94} Pt _{0.07} Rh _{0.01})Σ1.02(Hg _{0.85} Cu _{0.06} Fe _{0.06} Ni _{0.01})Σ0.98	-	-
20	-	Pd _{1.01} (Hg _{0.80} Cu _{0.12} Fe _{0.05} Te _{0.01})Σ0.98	-	-
21	Botryoidal and other alluvial grains, Córrego Bom Sucesso streams, Minas Gerais, Brazil	(Pd _{1.11} Pt _{0.01})Σ1.12(Hg _{0.79} Au _{0.09})Σ0.88	-	Fleet et al., 2002 [23]
22	-	Pd _{1.06} (Hg _{0.67} Au _{0.28})Σ0.95	-	-
23	-	Pd _{1.18} (Hg _{0.65} Au _{0.17})Σ0.82	-	-
24	-	Pd _{1.03} (Hg _{0.78} Au _{0.19})Σ0.97	-	Cabral et al., 2009 [68]
25	-	Pd _{1.09} (Hg _{0.84} Au _{0.07})Σ0.91	-	-

Note. The formulae are based on a total of two atoms per formula unit (a.p.f.u.).

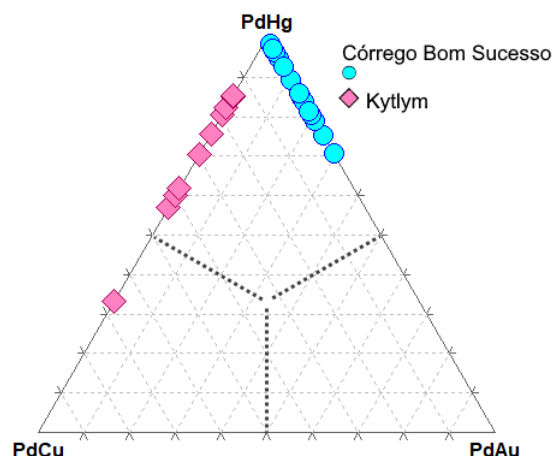


Figure 9. Compositional series of cupriferous and auriferous potarite, shown in PdCu–PdHg–PdAu compositional space (molar proportions). The two series are inferred on the basis of compositional data reported from the Kytlym complex, Urals, Russia, by Volchenko, 2011 [38] and Zaccarini et al., 2011 [66], and from Córrego Bom Sucesso, Minas Gerais, Brazil, by Fleet et al., 2002 [23] and Cabral et al., 2009 [68], respectively.

Table 9. Comparison of unit-cell parameters reported for various minerals and synthetic compounds related to unnamed Pt(Cu_{0.67}Sn_{0.33}), all in space group P4/mmm.

#	Mineral or Synthetic Compound Formula	Unit-Cell Parameters	References
1	Tulameenite; Pt ₂ CuFe	$a = 3.891(2)$, $c = 3.577(2)$ Å	Cabri et al., 1973 [3] IMA1972-016
2	Tulameenite revised; Pt(Cu _{0.5} Fe _{0.5})	$a = 2.7477(4)$, $c = 3.5870(8)$ Å	Bayliss, 1990 [18]
3	Tetraferroplatinum; PtFe	$a = 3.850(5)$, $c = 3.693(6)$ Å	Cabri and Feather, 1975 [4] IMA1974-012b
4	Tetraferroplatinum revised; PtFe	$a = 2.7235(10)$, $c = 3.720(3)$ Å	Bayliss, 1990 [18]
5	Ferronickelplatinum; Pt ₂ FeNi	$a = 3.871(4)$, $c = 3.635(5)$ Å	Rudashevskiy et al., 1983 [26] IMA1982-071
6	Ferronickelplatinum revised; Pt(Ni _{0.5} Fe _{0.5})	$a = 2.731(3)$, $c = 3.641(8)$ Å	Bayliss, 1990 [18]
7	Synthetic PtNi	$a = 2.711$, $c = 3.602$ Å	Leroux et al., 1988 [16]
8	Synthetic PtCo	$a = 2.698$, $c = 3.71$ Å	Leroux et al., 1988 [16]
9	Unnamed Pt(Cu _{0.67} Sn _{0.33})	$a = 2.838(3)$, $c = 3.650(4)$ Å	This study
10	Synthetic Pt(Cu _{0.67} Sn _{0.33})	$a = 2.82205(1)$, $c = 3.63637(2)$ Å	Juarez-Arellano et al., 2020 [1]
11	Tetra-auricupride; Au _{1.01} Cu _{0.99}	$a = 2.81$, $c = 3.72$ Å	Chen et al., 1982 [24]
12	Tetra-auricupride revised; AuCu	$a = 2.800$, $c = 3.670$ Å	Bayliss, 1990 [18]
13	Tetra-auricupride (platiferous); (Au _{0.80} Pt _{0.21}) _{Σ1.01} Cu _{1.00}	$a = 2.790(1)$, $c = 3.641(4)$ Å	Barkov et al., 2019 [10]
14	Synthetic AuCu(I)	$a = 2.785$ – 2.810 , $c = 3.671$ – 3.712 Å	Okamoto et al., 1987 [15]
15	Potarite; PdHg	$a = 3.02$, $c = 3.706$ Å	Spencer, 1928 [19]

4.6. The PdHg–PtHg Series

In addition, potarite displays a considerable extent of solid solution with PtHg, also having an AuCu-type structure ([65] and references therein). The existence of a new and Pt-dominant member is implied by compositions reported from vein-like pegmatitic ores of the Butyrinskoye (Butyrin) deposit, Kytlym complex, Urals, Russia [66]. Indeed, one of these compositions is notably Pt-rich, with a Pt/Pd ratio of 0.9 (#16, Table 8). Nineteen data points provided by the authors gave values of the atomic ratio (Pd + Pt)/(Hg + Cu + Fe + Ni + Sb) ranging 0.9 to 1.2, with a mean of 1.0.

4.7. The AuCu–PtCu Series

Tetra-auricupride, AuCu, forms a well-established series toward “PtCu” (Figure 10) on the basis of compositions reported from the Tulameen complex, British Columbia, Canada [12], the Sotajoki area, Finland [13], the Zolotaya River placer, western Sayans, Russia [11], lode and placer occurrences associated with the Kondyor complex, Khabarovskiy kray, Russia [14,70], the Noril’sk complex [71], and the River Bolshoy Khailyk placer, western Sayans, Russia [10]. In the latter occurrence, a platiniferous variant of tetra-auricupride contains up to ~30 mol.% of the “PtCu” component without significant modification of the unit cell. Its parameters are $a = 2.790(1)$, $c = 3.641(4)$ Å, with $c/a = 1.305$ [10], which are close to those reported for PtFe-type species [18] or parameters established for ordered AuCu(I) (#2, 14, Table 9).

The grains reported from Sotajoki and Noril’sk are substantially enriched in Pd (0.13–0.18 a.p.f.u.; #2, 9, Table 8). The total content of Pt + Pd attains 0.4 a.p.f.u. in the compound from Sotajoki (Figure 10).

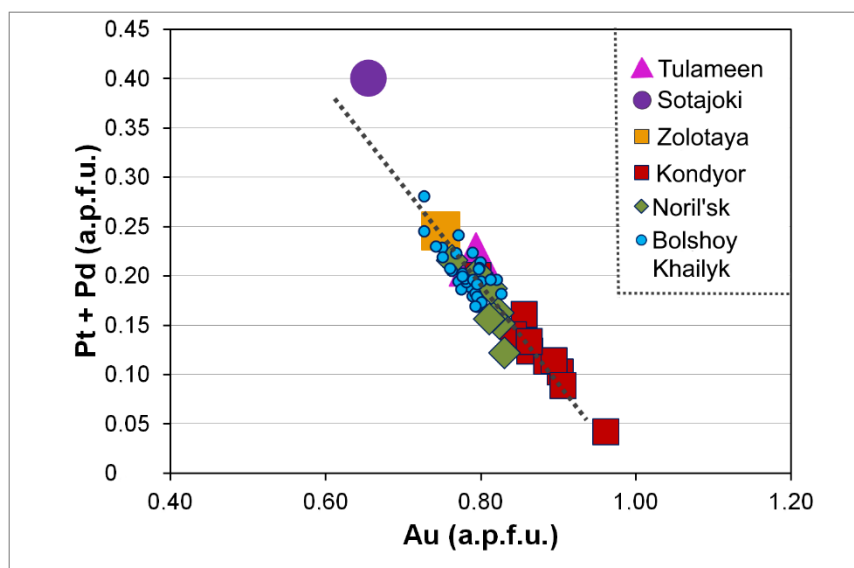


Figure 10. A plot of Au versus (Pt + Pd) in terms of atoms per formula unit (a.p.f.u.) showing the compositional series of platiniferous tetra-auricupride, which is documented on the basis of compositions reported from the Tulameen complex, British Columbia, Canada (Cabri and Laflamme, 1981 [12]), the Sotajoki area, Finland (Törnroos and Vuorelainen, 1987 [13]), the Zolotaya River placer, western Sayans, Russia (Tolstykh et al., 1997 [11]), lode and placer occurrences associated with the Kondyor complex, Khabarovskiy kray, Russia (Shcheka et al., 2004 [70], Nekrasov et al., 2005 [14]), the Noril’sk complex (Spiridonov, 2010 [71]), and from the River Bolshoy Khailyk placer, western Sayans, Russia (Barkov et al., 2019 [10]).

4.8. A Comparison of Unit-Cell Parameters

The various members of the group display a notable similarity in their unit-cell parameters, values of which were reported or revised as follows: tulameenite, $\text{Pt}(\text{Cu}_{0.5}\text{Fe}_{0.5})$, $a = 2.7477(4)$ and $c = 3.5870(8)$ Å (#2, Table 9); tetraferroplatinum, PtFe, $a = 2.7235(10)$ and

$c = 3.720(3)$ Å (#4, Table 4); ferronickelplatinum, $\text{Pt}(\text{Ni}_{0.5}\text{Fe}_{0.5})$, $a = 2.731(3)$ and $c = 3.641(8)$ Å (#6, Table 9) (cf. synthetic PtNi: $a = 2.711$ and $c = 3.602$ Å; #7, Table 9); tetra-auricupride, AuCu , $a = 2.800$ and $c = 3.670$ Å (#12, Table 9) (cf. platiniferous tetra-auricupride: $a = 2.790(1)$ and $c = 3.641(4)$ Å (#13, Table 9)); unnamed $\text{Pt}(\text{Cu}_{0.67}\text{Sn}_{0.33})$, $a = 2.838(3)$ and $c = 3.650(4)$ Å (#9, Table 9) (cf. synthetic analogue of the latter with $a = 2.82205(1)$ and $c = 3.63637(2)$ Å; [1]; and potarite, PdHg , $a = 3.02$ and $c = 3.706$ Å (#15, Table 9)).

The revision proposed by [18] involves a different setting of the cell (e.g., $3.891 \approx \sqrt{2} * 2.7477$; #1, 2, Table 9). The powder XRD pattern simulated on the basis of the structure data of [18] is identical to the powder data reported by [4]. The different setting is also provided for tetra-auricupride, AuCu , with a revision of space group to $P4/mmm$; the $C4/mmm$ symmetry proposed previously is a multiple cell of $P4/mmm$ (#11, 12, Table 9). This revision is consistent with characteristics of the AuCu(I) phase, $P4/mmm$, $a = 2.785\text{--}2.810$ Å and $c = 3.671\text{--}3.712$ Å [15].

5. Concluding Comments and Principles of Future Classification

The unnamed species of PGM investigated at Bolshoy Khailyk is analogous, both compositionally and structurally, to synthetic $\text{Pt}(\text{Cu}_{0.67}\text{Sn}_{0.33})$ obtained and characterized by Juarez-Arellano et al. [2]. It represents a member of a large family of isostructural members that have similar unit-cell parameters and conform to the space group $P4/mmm$. These species and their variants are composed of several participating elements (Pt, Pd, Ir, Au) vs. (Fe, Cu, Ni, Sn, Sb, Hg, Au), some of which (e.g., Au) can probably occupy more than a single site in the structure. Considerable extents of mutual solid-solution exist among the inferred end-members in these series. Consequently, new members can reasonably be expected in accordance with the 50% rule.

Five members of the group are presently recognized: *Tetraferroplatinum*, PtFe [5]; cf. [18], is most abundant as the Fe-dominant representative of the extensive field of complex solid-solutions occurring in the system PtNi–PtFe–PtCu (cf. Figures 5 and 6). *Tulameenite*, Pt_2CuFe [4], and its synthetic analogue appear to have an ordered face-centered tetragonal structure stabilized below a temperature of ~ 1178 °C as a result of an ordering transformation [72]. Similarly, *ferronickelplatinum* Pt_2NiFe [26] forms as a result of a phase transformation implied for synthetic PtNi in the system Pt–Ni, cf. [73]. This mode of origin is consistent with the transformation $\text{AuCu(II)} \rightarrow (\text{AuCuI})$ in the system Au–Cu [15]. On the other hand, according to the suggestion of [18], these species may represent intermediate members, i.e., $\text{Pt}(\text{Cu}_{0.5}\text{Fe}_{0.5})$ and $\text{Pt}(\text{Ni}_{0.5}\text{Fe}_{0.5})$ (#2, 6, Table 7). In addition, the Ni-dominant phases reported (#1, 12, 13, Table 7; [38,52,57]) are likely related to synthetic PtNi (#7, Table 9; [16]). The unnamed mineral [$\text{Pt}(\text{Cu}_{0.67}\text{Sn}_{0.33})$] described here may represent the Cu-dominant member of the group; by analogy, different compositional variants could occur in the systems PtCu–PtSn and PtNi–PtFe–PtCu (cf. Figure 5), among others. *Tetra-auricupride*, the next member, is ideally AuCu [24], cf. [18], though it can display considerable extents of Pt-for-Au and Pd-for-Au substitutions (Figure 10). *Potarite*, ideally PdHg [19], forms three series of compositions: platiniferous, auriferous, and cupriferous (#12–20, Table 8, Figure 9). There is no doubt that several other members of the group will be documented in future.

The intermetallic compounds or alloys related to tetraferroplatinum and tulameenite can be better grouped (R. Miyawaki, written commun.; Figures 11 and 12) on the basis of the degree of order of metals in terms of $Fm\bar{3}m$ (#225), $Pm\bar{3}m$ (#221), $P4/mmm$ (#123) ‘tP4’, $C4/mmm$ (a multiple cell of the smaller $P4/mmm$), ‘tP2’, among other possibilities. It is thus necessary to clarify the degree of order of the metal atoms in these minerals in order to establish in each case the true space-group of the unit cell. If the crystal structures of the polymorphs have essentially the same topology, differing only in terms of a structural distortion or in the degree of order of some of the atoms comprising the structure, such polymorphs are not regarded as separate species [74]. Thus, on the basis of the literature data on valid mineral species making up the potential group(s), the species can be classified into two types. (1) ABC_2 type, with an ordered distribution of metal

atoms in the tetragonal system, space group $P4/mmm$, 'tP4'. The members are tulameenite Pt_2CuFe , $P4/mmm$, $a = 3.89$, and $c = 3.58$ Å [3], and ferronickelplatinum Pt_2FeNi , $P4/mmm$, $a = 3.871$, and $c = 3.635$ Å [26]. (2) AB type, with a disordered distribution of metal atoms in the tetragonal system ($P4/mmm$), 'tP2'. The members are tetraferroplatinum $PtFe$, $P4/mmm$, $a = 2.724$, $c = 3.702$ Å [25], tetra-auricupride $CuAu$, $P4/mmm$, $a = 2.81$, $c = 3.72$ Å [24], and unnamed $Pt(Cu_{0.67}Sn_{0.33})$, $P4/mmm$, $a = 2.838$, and $c = 3.650$ Å (this study), among others.

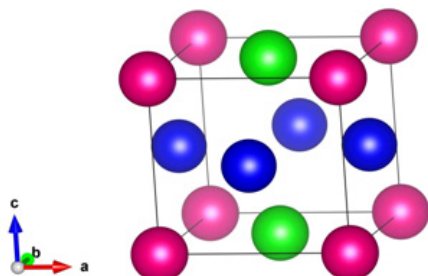


Figure 11. A general scheme proposed for ABC_2 -type compounds on the basis of an ordered distribution of metal atoms in the 'tP4' structure. The colored spheres represent the A (blue), B (green) and C (magenta) atoms.

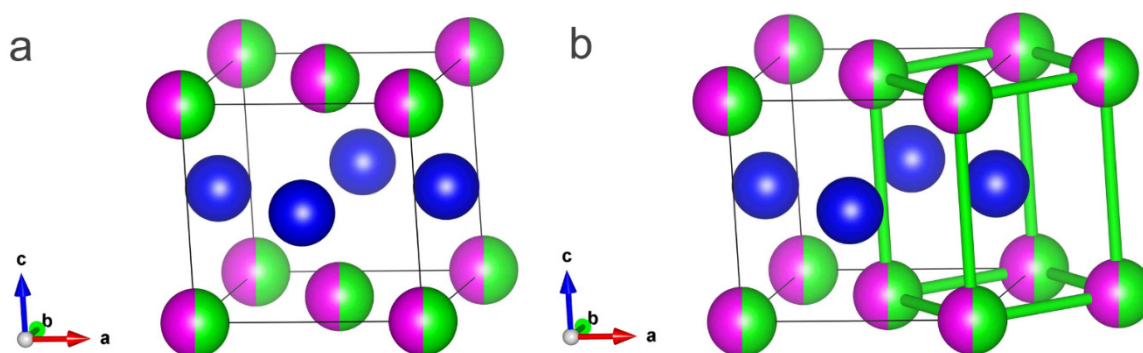


Figure 12. Schemes for AB-type compounds involving a disordered distribution of metal atoms in the 'tP4' (a; left) and 'tP2' (b; right) structures. The bicolored spheres schematically represent the disordered distribution of the A and B atoms at one site; the blue spheres represent the C atoms at the other site.

Author Contributions: The authors wrote the article together. A.Y.B., R.F.M.: data analysis, interpretations, conclusions, writing; L.B.: XRD study, discussions, writing; E.A.J.-A.: synthesis, characterization of synthetic analogue, discussions, writing; N.T.: Synchrotron X-ray micro-Laue diffraction study, writing; C.M.: electron backscatter diffraction (EBSD) study, writing; G.I.S.: regional investigation, sampling, writing. All authors have read and agreed to the published version of the manuscript.

Funding: This research received no specific grant.

Data Availability Statement: The data are available upon a reasonable request (from A.Y.B.).

Acknowledgments: We thank Ritsuro Miyawaki, Chairman, Commission on New Minerals, Nomenclature and Classification (CNMNC), IMA, for generously sharing his ideas on the general principles of nomenclature involving the $Pt(Cu_{0.67}Sn_{0.33})$ mineral that we have investigated. This research used beamline 12.3.2 at the Advanced Light Source, which is a DOE Office of Science User Facility under contract no. DE-AC02-05CH11231. A.Y.B. acknowledges that this study was also supported in part by the Russian Foundation for Basic Research (project # RFBR 19-05-00181). A support from the Cherepovets State University is gratefully acknowledged (A.Y.B.). We are grateful to B. Winkler and W. Morgenroth for their contributions in characterization of the synthetic equivalent, and to S.A. Silyanov for the reflectance measurements. We thank the Editorial board members and two anonymous referees for their constructive comments.

Conflicts of Interest: The authors declare no conflict of interest.

References

1. Barkov, A.Y.; Shvedov, G.I.; Silyanov, S.A.; Martin, R.F. Mineralogy of platinum-group elements and gold in the ophiolite-related placer of the River Bolshoy Khailyk, western Sayans, Russia. *Minerals* **2018**, *8*, 247. [[CrossRef](#)]
2. Juarez-Arellano, E.A.; Schellhase, S.; Morgenroth, W.; Binck, J.; Tamura, N.; Stan, C.; Spahr, D.; Bayarjargal, L.; Barkov, A.; Milman, V.; et al. Synthesis and characterization of Pt(Cu_{0.67}Sn_{0.33}). *Solid State Sci.* **2020**, *105*, 106282. [[CrossRef](#)]
3. Barkov, A.Y.; Martin, R.F.; Poirier, G.; Tarkian, M.; Pakhomovskii, Y.A.; Men'shikov, Y.P. Tatyanaite, a new platinum-group mineral, the Pt analogue of taimyrite, from the Noril'sk complex (northern Siberia, Russia). *Eur. J. Miner.* **2000**, *12*, 391–396. [[CrossRef](#)]
4. Cabri, L.J.; Owens, D.R.; Laflamme, J.H.G. Tulameenite, a new platinum—iron—copper mineral from placers in the Tulameen River area, British Columbia. *Can. Miner.* **1973**, *12*, 21–25.
5. Cabri, L.J.; Feather, C.E. Platinum-iron alloys: A nomenclature based on a study of natural and synthetic alloys. *Can. Miner.* **1975**, *13*, 117–126.
6. Barkov, A.Y.; Cabri, L.J. Variations of major and minor elements in Pt–Fe alloy minerals: A review and new observations. *Minerals* **2019**, *9*, 25. [[CrossRef](#)]
7. Tamura, N. XMAS: A versatile tool for analyzing synchrotron X-ray microdiffraction data. In *Strain and Dislocation Gradients from Diffraction*; Barabash, R., Ice, G., Eds.; Imperial College Press: London, UK, 2014; pp. 125–155.
8. Boulouf, A.; Louër, D. Powder pattern indexing with the dichotomy method. *J. Appl. Crystallogr.* **2004**, *37*, 724–731. [[CrossRef](#)]
9. Rodriguez-Carvajal, J. Recent advances in magnetic structure determination by neutron powder diffraction. *Phys. B* **1993**, *192*, 55–69. [[CrossRef](#)]
10. Barkov, A.Y.; Tamura, N.; Shvedov, G.I.; Stan, C.V.; Ma, C.; Winkler, B.; Martin, R.F. Platiniferous tetra-auricupride: A case study from the Bolshoy Khailyk placer deposit, western Sayans, Russia. *Minerals* **2019**, *9*, 160. [[CrossRef](#)]
11. Tolstykh, N.D.; Krivenko, A.P.; Pospelova, L.N. Unusual compounds of iridium, osmium and ruthenium with selenium, tellurium and arsenic from placers of the Zolotaya River (western Sayans). *Zap. Vseross. Miner. Obshch.* **1997**, *126*, 23–34. (In Russian)
12. Cabri, L.J.; Laflamme, J.H.G. Analyses of minerals containing platinum-group elements. In *Platinum-Group Elements: Mineralogy, Geology, Recovery*; Cabri, L.J., Ed.; Canadian Institute of Mining and Metallurgy: Montreal, QC, Canada, 1981; Special Volume 23, pp. 151–173.
13. Törnroos, R.; Vuorelainen, Y. Platinum-group metals and their alloys in nuggets from alluvial deposits in Finnish Lapland. *Lithos* **1987**, *20*, 491–500. [[CrossRef](#)]
14. Nekrasov, I.Y.; Lennikov, A.M.; Zalizhchak, B.L.; Oktyabry, R.A.; Ivanov, V.V.; Sapin, V.I.; Taskaev, V.I. Compositional variations in platinum-group minerals and gold, Konder alkaline-ultrabasic massif, Aldan Shield, Russia. *Can. Miner.* **2005**, *43*, 637–654. [[CrossRef](#)]
15. Okamoto, H.; Chakrabarti, D.J.; Laughlin, D.E.; Massalski, T.B. The Au–Cu (gold–copper) system. *J. Phase Equilibria* **1987**, *8*, 454–474. [[CrossRef](#)]
16. Leroux, C.; Cadeville, M.C.; Pierron-Bohnes, V.; Inden, G.; Hinz, F. Comparative investigation of structural and transport properties of L1₀ NiPt and CoPt phases; the role of magnetism. *J. Phys. F Met. Phys.* **1988**, *18*, 2033–2051. [[CrossRef](#)]
17. Nixon, G.; Cabri, L.J.; Laflamme, J.H.G. Platinum-group-element mineralization in lode and placer deposits associated with the Tulameen Alaskan-type complex, British Columbia. *Can. Miner.* **1990**, *28*, 503–535.
18. Bayliss, P. Revised unit-cell dimensions, space group, and chemical formula of some metallic minerals. *Can. Miner.* **1990**, *28*, 751–755.
19. Spencer, L.J. Potarite, a new mineral discovered by the late Sir John Harrison in British Guiana. *Miner. Mag.* **1928**, *21*, 397–406. [[CrossRef](#)]
20. Bittner, H.; Nowotny, H. Zur Kenntnis des Systems: Palladium–Quecksilber. *Mon. Chem.* **1952**, *83*, 287–289. [[CrossRef](#)]
21. Terada, K.; Cagle, F.W., Jr. The crystal structure of potarite (PdHg) with some comments on allopalladium. *Am. Mineral.* **1960**, *45*, 1093–1097.
22. Cummins, J.D.; Berndt, A.F. A single crystal study of palladium-mercury and γ mercury–tin. *J. Less-Common Met.* **1969**, *19*, 431–432. [[CrossRef](#)]
23. Fleet, M.E.; De Almeida, C.M.; Angeli, N. Botryoidal platinum, palladium and potarite from the Bom Sucesso stream, Minas Gerais, Brazil: Compositional zoning and origin. *Can. Miner.* **2002**, *40*, 341–355. [[CrossRef](#)]
24. Chen, K.; Yu, T.; Zhang, Y.; Peng, Z. Tetra-auricupride, CuAu discovered in China. *Sci. Geol. Sin.* **1982**, *17*, 111–116. (In Chinese, English Abstract).
25. Cabri, L.J.; Rosenzweig, A.; Pinch, W.W. Platinum-group minerals from Onverwacht. I. Pt–Fe–Cu–Ni alloys. *Can. Miner.* **1977**, *15*, 380–384.
26. Rudashevskiy, N.S.; Mochalov, A.G.; Men'shikov, Y.P.; Shumskaya, N.I. Ferronickelplatinum, Pt₂FeNi, a new mineral species. *Zap. Vses. Mineral. Obshch.* **1983**, *112*, 487–494. (In Russian)
27. Yu, Z. New data on hongshiite. *Bull. Inst. Geol. Chin. Acad. Geol. Sci.* **1982**, *4*, 75–81, Abstract in *Am. Miner.* **1984**, *69*, 411–412. (In Chinese with English Abstract).
28. Yu, Z. New data of daomanite and hongshiite. *Acta Geol. Sin.* **2001**, *75*, 458–466.
29. Wyckoff, R.W.G. *Structure of Crystals*, 2nd ed.; The Chemical Catalog Company, Inc.: New York, NY, USA, 1931.

30. Cabri, L.J.; Harris, D.C.; Weiser, T. Mineralogy and distribution of platinum-group mineral (PGM) placer deposits of the world. *Explor. Mining Geol.* **1996**, *5*, 73–167.
31. Tolstykh, N.D.; Foley, J.Y.; Sidorov, E.G.; Laajoki, K.V.O. Composition of the platinum-group minerals in the Salmon River placer deposit, Goodnews Bay, Alaska. *Can. Miner.* **2002**, *40*, 463–471. [[CrossRef](#)]
32. Cabri, L.J.; Genkin, A.D. Re-examination of Pt alloys from lode and placer deposits, Urals. *Can. Miner.* **1991**, *29*, 419–425.
33. Garuti, G.; Pushkarev, E.V.; Zaccarini, F. Composition and paragenesis of Pt alloys from chromitites of the Uralian Alaskan-type Kytlym and Uktus complexes, northern and central Urals, Russia. *Can. Miner.* **2002**, *40*, 1127–1146. [[CrossRef](#)]
34. Garuti, G.; Pushkarev, E.V.; Zaccarini, F.; Cabella, R.; Anikina, E. Chromite composition and platinum-group mineral assemblage in the Uktus Uralian-Alaskan-type complex (Central Urals, Russia). *Miner. Depos.* **2003**, *38*, 312–326. [[CrossRef](#)]
35. Augé, T.; Genna, A.; Legendre, O.; Ivanov, K.S.; Volchenko, Y.A. Primary platinum mineralization in the Nizhny Tagil and Kachkanar ultramafic complexes, Urals, Russia: A genetic model for PGE concentration in chromite-rich zones. *Econ. Geol.* **2005**, *100*, 707–732. [[CrossRef](#)]
36. Tolstykh, N.D.; Telegin, Y.M.; Kozlov, A.P. Platinum mineralization of the Svetloborsky and Kamenushinsky massifs (Urals Platinum Belt). *Russ. Geol. Geophys.* **2011**, *52*, 603–619. [[CrossRef](#)]
37. Tolstykh, N.; Kozlov, A.; Telegin, Y. Platinum mineralization of the Svetly Bor and Nizhny Tagil intrusions, Ural Platinum Belt. *Ore Geol. Rev.* **2015**, *67*, 234–243. [[CrossRef](#)]
38. Volchenko, Y.A. *Platinum of the Urals 2*; The Russian Academy of Sciences, Ural Branch: Ekaterinburg, Russia, 2011. (In Russian)
39. Zaccarini, F.; Pushkarev, E.; Garuti, G.; Krause, J.; Dvornik, G.P.; Stanley, C.; Bindi, L. Platinum-group minerals (PGM) nuggets from alluvial-eluvial placer deposits in the concentrically zoned mafic-ultramafic Uktus complex (central Urals, Russia). *Eur. J. Miner.* **2013**, *25*, 519–531. [[CrossRef](#)]
40. Barannikov, A.G.; Osovetskiy, B.M. Platinum, platinum placers of the Urals and criteria and features of their spatial association with the primary sources. *News Ural. State Min. Univ.* **2014**, *3*, 12–28. (In Russian)
41. Stepanov, S.Y. A comparative characteristic of platinum mineralization in the Svetloborsky, Veresoborsky, and Nizhnetagil'sky dunite-clinopyroxenite intrusives (Middle Urals, Russia). *New Data Miner.* **2015**, *50*, 29–37. (In Russian)
42. Malitch, K.N.; Badanina, I.Y. Iron-platinum alloys from chromitites of the Nizhny Tagil and Kondyor clinopyroxenite-dunite massifs (Russia). *Dokl. Earth Sci.* **2015**, *462*, 634–637. [[CrossRef](#)]
43. Palamarchuk, R.S.; Stepanov, S.Y.; Khanin, D.A.; Antonov, A.V. Platinum mineralization in massive chromitites of the Iovskiy dunite body (northern Urals). *Mosc. Univ. Geol. Bull.* **2017**, *5*, 68–76. (In Russian)
44. Tolstykh, N.D.; Sidorov, E.G.; Laajoki, K.V.O.; Krivenko, A.P.; Podlipskiy, M. The association of platinum-group minerals in placers of the Pustaya River, Kamchatka, Russia. *Can. Miner.* **2000**, *38*, 1251–1264. [[CrossRef](#)]
45. Malitch, K.N.; Thalhammer, O.A.R. Pt-Fe nuggets derived from clinopyroxenite-dunite massifs, Russia: A structural, compositional and osmium-isotope study. *Can. Miner.* **2002**, *40*, 395–418. [[CrossRef](#)]
46. Sidorov, E.G.; Tolstykh, N.D.; Podlipskiy, M.Y.; Pakhomov, I.O. Placer PGE minerals from the Filippa clinopyroxenite-dunite massif (Kamchatka). *Russ. Geol. Geophys.* **2004**, *45*, 1080–1097.
47. Sidorov, E.G.; Kozlov, A.P.; Tolstykh, N.D. *The Gal'moenan Basic-Ultrabasic Massif and its Platinum Potential*; Nauchnyi Mir: Moscow, Russia, 2012. (In Russian)
48. Yakovlev, Y.N.; Mitrofanov, F.P.; Razhev, S.A.; Veselovsky, N.N.; Distler, V.V.; Grokhovskaya, T.L. Mineralogy of PGE in the mafic-ultramafic massifs of the Kola region. *Miner. Petrol.* **1991**, *43*, 181–192. [[CrossRef](#)]
49. Rudashevsky, N.S.; Avdontsev, S.N.; Dneprovskaya, M.B. Evolution of PGE mineralization in hortonolitic dunites of the Mooihoek and Onverwacht pipes, Bushveld Complex. *Miner. Petrol.* **1992**, *47*, 37–54. [[CrossRef](#)]
50. Barkov, A.Y.; Lednev, A.I. A rhenium-molybdenum-copper sulfide from the Lukkulaivaara layered intrusion, northern Karelia, Russia. *Eur. J. Miner.* **1993**, *5*, 1227–1234. [[CrossRef](#)]
51. Grokhovskaya, T.L.; Lapina, M.I.; Ganin, V.A.; Grinevich, N.G. PGE mineralization in the Burakovskiy layered complex, southern Karelia, Russia. *Geol. Ore Depos.* **2005**, *47*, 283–308.
52. Melcher, F.; Oberthür, T.; Lodziak, J. Modification of detrital platinum-group minerals from the eastern Bushveld complex, South Africa. *Can. Miner.* **2005**, *43*, 1711–1734. [[CrossRef](#)]
53. Oberthür, T.; Weiser, T.W.; Melcher, F.; Gast, L.; Wöhr, C. Detrital platinum-group minerals in rivers draining the Great Dyke, Zimbabwe. *Can. Miner.* **2013**, *51*, 197–222. [[CrossRef](#)]
54. Oberthür, T.; Junge, M.; Rudashevsky, N.; de Meyer, E.; Gutter, P. Platinum-group minerals in the LG and MG chromitites of the eastern Bushveld Complex, South Africa. *Miner. Depos.* **2016**, *51*, 71–87. [[CrossRef](#)]
55. Barkov, A.Y.; Shvedov, G.I.; Martin, R.F. PGE-(REE-Ti)-rich micrometer-sized inclusions, mineral associations, compositional variations, and a potential lode source of platinum-group minerals in the Sisim Placer Zone, eastern Sayans, Russia. *Minerals* **2018**, *8*, 181. [[CrossRef](#)]
56. Tolstykh, N.; Sidorov, E.; Kozlov, A. Platinum-group minerals from the Ol'khovaya-placers related to the Karaginsky ophiolite complex, Kamchatskiy Mys Peninsula, Russia. *Can. Miner.* **2009**, *47*, 1057–1074. [[CrossRef](#)]
57. Agafonov, L.V.; Kuzhuget, K.S.; Oydup, C.K.; Stupakov, S.I. *Native Metals in Ultrabasic-Basic Rocks of Tuva*; Velinskiy, V.V., Ed.; United Institute of Geology, Geophysics and Mineralogy, SB RAS: Novosibirsk, Russia, 1993; 86p. (In Russian)
58. Cook, N.J.; Ciobanu, C.L.; Merkle, R.K.W.; Bernhardt, H.-J. Sobolevskite, taimyrite, and Pt₂CuFe (tulameenite?) in complex massive talnakhite ore, Noril'sk orefield, Russia. *Can. Miner.* **2002**, *40*, 329–340. [[CrossRef](#)]

59. Barkov, A.Y.; Tarkian, M.; Laajoki, K.V.O.; Gehör, S.A. Primary platinum-bearing copper from the Lesnaya Varaka ultramafic alkaline complex, Kola Peninsula, northwestern Russia. *Miner. Petrol.* **1998**, *62*, 61–72. [[CrossRef](#)]
60. Neradovsky, Y.N.; Groshev, N.Y.; Voytekhovskiy, Y.L.; Borozdina, S.V.; Savchenko, E.E. Minerals of platinum, palladium, silver, and gold of the Por'yerechensky titanium-bearing complex (Kola Peninsula). *Her. Kola Sci. Cent. RAS* **2017**, *3*, 71–87. (In Russian)
61. Laflamme, J.H.G. *Mineralogical Study of Platinum-Group Minerals from Au–Pt-Bearing Placer Samples from British Columbia*; Report MMSL 02-038(CR): Appendix “Electron Microprobe Data”; CANMET Mining and Mineral Sciences Laboratories: Ottawa, ON, Canada, 2002; pp. A-1–A-19.
62. Barkov, A.Y.; Fleet, M.E.; Nixon, G.T.; Levson, V.M. Platinum-group minerals from five placer deposits in British Columbia, Canada. *Can. Miner.* **2005**, *43*, 1687–1710. [[CrossRef](#)]
63. Barkov, A.Y.; Martin, R.F.; Fleet, M.E.; Nixon, G.T.; Levson, V.M. New data on associations of platinum-group minerals in placer deposits of British Columbia, Canada. *Miner. Petrol.* **2008**, *92*, 9–29. [[CrossRef](#)]
64. Pušelj, M.; Ban, Z. Preparation and crystal structure of NiHg. *Z. Nat. B* **1977**, *32*, 479. [[CrossRef](#)]
65. Souza, G.R.; Pastre, I.A.; Benedetti, A.V.; Ribeiro, C.A.; Fertoni, F.L. Solid state reactions in the platinum–mercury system. *J. Therm. Anal. Calorim.* **2007**, *88*, 127–132. [[CrossRef](#)]
66. Zaccarini, F.; Garuti, G.; Pushkarev, E.V. Unusually PGE-rich chromitite in the Butyrin vein of the Kytlym Uralian-Alaskan complex, northern Urals, Russia. *Can. Miner.* **2011**, *49*, 1413–1431. [[CrossRef](#)]
67. Bindi, L.; Zaccarini, F.; Garuti, G.; Angeli, N. The solid solution between platinum and palladium in nature. *Miner. Mag.* **2013**, *77*, 269–274. [[CrossRef](#)]
68. Cabral, A.R.; Vymazalová, A.; Lehmann, B.; Tupinambá, M.; Haloda, J.; Laufek, F.; Vlek, V.; Kwitko-Ribeiro, R. Poorly crystalline Pd–Hg–Au intermetallic compounds from Corrego Bom Sucesso, southern Serra do Espinhaco, Brazil. *Eur. J. Miner.* **2009**, *21*, 811–816. [[CrossRef](#)]
69. Rudashevsky, N.S.; McDonald, A.M.; Cabri, L.J.; Nielsen, T.F.D.; Stanley, C.J.; Kretzer, Y.L.; Rudashevsky, V.N. Skaergaardite, PdCu, a new platinum-group intermetallic mineral from the Skaergaard intrusion, Greenland. *Miner. Mag.* **2004**, *68*, 615–632. [[CrossRef](#)]
70. Shcheka, G.G.; Lehmann, B.; Gierth, E.; Gomann, K.; Wallianos, A. Macrocystals of Pt–Fe alloy from the Kondyor PGE placer deposit, Khabarovskiy kray, Russia: Trace-element content, mineral inclusions and reaction assemblages. *Can. Miner.* **2004**, *42*, 601–617. [[CrossRef](#)]
71. Spiridonov, E.M. Ore-magmatic systems of the Noril'sk ore field. *Russ. Geol. Geophys.* **2010**, *51*, 1059–1077. [[CrossRef](#)]
72. Shahmiri, M.; Murphy, S.; Vaughan, D.J. Structural and phase equilibria studies in the system Pt–Fe–Cu and the occurrence of tulameenite (Pt₂FeCu). *Miner. Mag.* **1985**, *49*, 547–554. [[CrossRef](#)]
73. Lyakishev, N.P. (Ed.) *Phase Diagrams of Binary Metallic Systems*; 3 Volumes; Mashinostroenie: Moscow, Russia, 2001; p. 627. (In Russian)
74. Nickel, E.H.; Grice, J.D. The IMA Commission on New Minerals and Mineral Names: Procedures and guidelines on mineral nomenclature, 1998. *Can. Miner.* **1998**, *36*, 913–926. [[CrossRef](#)]